POSSIBILITIES OF POLARIZATION CURRENT MODEL ANALYSIS FOR ANTENNAS CONSISTING OF DIELECTRIC MATERIALS

Takashi INOUE Naoki INAGAKI Nobuyoshi KIKUMA

Department of Electrical and Computer Engineering
Nagoya Institute of Technology
Gokiso-cho, Showa-ku, Nagoya 466-8555, Japan
E-mail takasun@maxwell.elcom.nitech.ac.jp

1 Introduction

Keeping step with the recent progress in mobile telecommunications, the frequency in use tends to be higher to provide the enough bandwidth for diverse services. Antennas for such applications need to be small,light weight and of simple structure. Dielectric resonator antennas have been studied as one of the candidate for these requirements.

Antennas consisting of materials including dielectric have been studied mainly by experiments. For the design of such antennas, the theoretical treatments are indispensable.

There are several numerical method solving the boundary value problems for the structure including dielectric. Finite Difference Time Domain (FDTD) Method , Finite Element Method, Boundary Element Method, and Volume Integral Equation Method are the representatives. This paper examines the Polarization Current Model Method (referred to as PCMM hereafter) concerning the possibilities to the numerical analysis of antennas including the dielectric materials. The PCMM was introduced by Richmond in 1960s. He published the papers dealing with the scattering by a dielectric cylinder of arbitrary cross section shape, for both the TM-wave incidence case[1], and the TE-wave incidence case[2].

The outline of the PCMM application to 2D problems will be described in the next section, where it is pointed out that some care should be paid. A dielectric loaded slot antenna is analyzed, and the results are compared with those by the HP-HFSS (High Frequency Structure Simulator) which belongs to the category of Finite Element Method.

2 Outline of Polarization Current Model Method

Maxwell equations inside the medium with relative permittivity ε_r can betransformed as follows.

$$\boldsymbol{\nabla}\times\boldsymbol{E}+j\omega\mu_0\boldsymbol{H}=\boldsymbol{0},\quad \boldsymbol{\nabla}\times\boldsymbol{H}-j\omega\varepsilon_0\boldsymbol{E}=\boldsymbol{J} \tag{1}$$

$$\boldsymbol{J}=j\omega\varepsilon_0(\varepsilon_r-1)\boldsymbol{E} \tag{2}$$

, where $\boldsymbol{J}$ is referred to as polarization current[1]. Eq.(1) is equivalent to the Maxwell's equation in the vacuum where $\boldsymbol{J}$ exists, which means that the scattered electromagnetic field by the dielectric body is equal to the electromagnetic field radiated from the current distribution $\boldsymbol{J}$. Hence, the total field $\boldsymbol{E}^t$, the incident field $\boldsymbol{E}^i$ and the scattered field $\boldsymbol{E}^s$ are equated as

$$\boldsymbol{E}^t = \boldsymbol{E}^i+\boldsymbol{E}^s \tag{3}$$

$$\boldsymbol{E}^s = k_0^2\int_V(\varepsilon_r-1)\boldsymbol{E}^t G\,dv'-\boldsymbol{\nabla}\int_V(\varepsilon_r-1)\boldsymbol{E}^t\cdot\boldsymbol{\nabla}G\,dv' \tag{4}$$

$$G = \frac{e^{-jk_0|\boldsymbol{r}-\boldsymbol{r}'|}}{4\pi|\boldsymbol{r}-\boldsymbol{r}'|} \tag{5}$$

Eq.(4) is an integral equation for the unknown total field $\boldsymbol{E}^t$, in which $\boldsymbol{r}$ is an observation point and $\boldsymbol{r}'$ is a source point, respectively.

Consider the 2D problem by the PCMM, where the fields are independent of y. For the TE^y polarized incident wave, Eq.(3) reduces to the following matrix equation in the moment method treatment of point matching procedure.

$$\begin{bmatrix} Z_{xx} & Z_{xz} \\ Z_{zx} & Z_{zz} \end{bmatrix} \begin{bmatrix} E_x^t \\ E_z^t \end{bmatrix} = \begin{bmatrix} E_x^i \\ E_z^i \end{bmatrix} \tag{6}$$

Here,

$$Z_{xx}^{nm} = \delta_{nm} - (\varepsilon_m - 1)\left(k_0^2 + \frac{\partial^2}{\partial x^2}\right)\int_{S_m} G dS' \tag{7}$$

$$Z_{xz}^{nm} = Z_{zx}^{nm} = -(\varepsilon_m - 1)\frac{\partial^2}{\partial x \partial z}\int_{S_m} G dS' \tag{8}$$

$$Z_{zz}^{nm} = \delta_{nm} - (\varepsilon_m - 1)\left(k_0^2 + \frac{\partial^2}{\partial z^2}\right)\int_{S_m} G dS' \tag{9}$$

$$G_{nm} = \frac{1}{4j}H_0^{(2)}(k_0|\boldsymbol{\rho}_n - \boldsymbol{\rho}'_m|) \tag{10}$$

ε_m is the relative permittivity of the discretized m-th subsegment, and $H_0^{(2)}(x)$ is the second kind Hankel function of order 0.

When the integral area S_m in Eqs.(7)$\sim$ (9) is a rectangular region as shown in Fig.1(a), it is convenient to replace it by the circular region as shown in Fig.1(b). By this approximation,

$$\begin{aligned} \int_{S_m} G_{nm} dS' &= \frac{1}{4j}\int_{S_m} H_0^{(2)}(k_0|\boldsymbol{\rho}_n - \boldsymbol{\rho}'_m|)dS' \\ &= \begin{cases} -\dfrac{j\pi}{2k_0^2}k_0 u J_1(k_0 u) H_0^{(2)}(k_0 R_{nm}) & (n \neq m) \\ -\dfrac{1}{k_0^2}\left\{\dfrac{j\pi}{2}k_0 u H_1^{(2)}(k_0 u) + 1\right\} & (n = m) \end{cases} \end{aligned} \tag{11}$$

, where $u = \dfrac{\ell}{\sqrt{\pi}}$, $R_{nm} = |\boldsymbol{\rho}_n - \boldsymbol{\rho}_m|$. Substituting Eq.(11) in Eqs.(7)$\sim$(9), and solving the Eq.(6), we obtain the total electric field $\boldsymbol{E}^t$.

During this analytical process, special care has to be paid to the differentiation of Eq.(11) when $n = m$, namely the case where the source point and the observation point coincides. The correct derivatives are as follows.

$$\frac{\partial^2}{\partial x^2}\int_{S_m} G dS' = \frac{\partial^2}{\partial z^2}\int_{S_m} G dS' = \frac{j\pi}{4}k_0 u H_1^{(2)}(k_0 u) \tag{12}$$

, which can be derived from the following relations and from the symmetrical property.

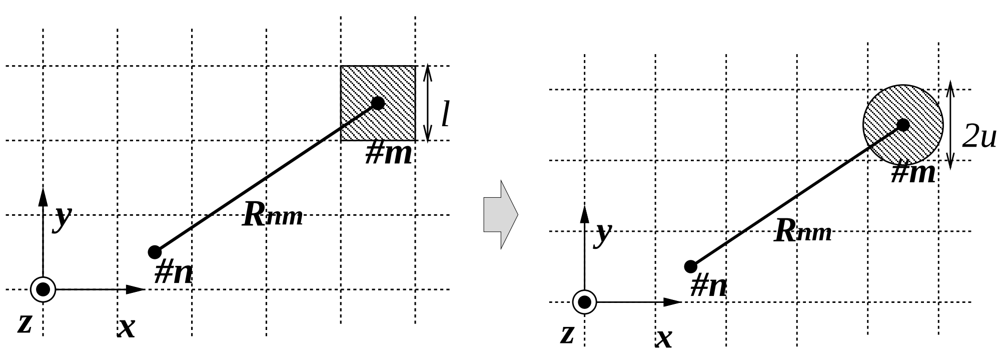

(a) The rectangular region of integration.

(b) The circular region of integration.

Figure 1: Transformation from the rectangular to the circular integral region

$$\left(\frac{\partial^2}{\partial x^2}+\frac{\partial^2}{\partial z^2}+k_0^2\right)G=-\delta(|\boldsymbol{\rho}-\boldsymbol{\rho}'|) \tag{13}$$

$$\int_{S_m}\left(\frac{\partial^2}{\partial x^2}+\frac{\partial^2}{\partial z^2}\right)GdS'=-1-k_0^2\int_{S_m}GdS'=\frac{j\pi}{2}k_0uH_1^{(2)}(k_0u) \tag{14}$$

3 Analysis of dielectric loaded slot antenna

Fig.2(a) shows a dielectric loaded slot antenna, where a slot with width s is placed on $x-y$ plane, one of the walls of a parallel plate waveguide, and a rectangular dielectric with width W and hight H is placed on the slot. The parallel plate waveguide is a kind of TEM waveguide, and the field is independent of y and no fringing field exists if it is infinite in extent in the y direction. For the thin slot, i.e. if s is much smaller than a wavelength, the electric field on the slot aperture can be approximated to be constant. For the uniform electric field $-E_x$,

$$\boldsymbol{M}=-E_x\hat{\boldsymbol{x}}\times\hat{\boldsymbol{z}}=\hat{\boldsymbol{y}}M_z \tag{15}$$

by the equivalence principle. Moreover, as the infinitely large conducting plate at $z=0$ may be removed according to the image theory, the structure of Fig.2(a) can be equivalently replaced by the structure of Fig.2(b), where the constant magnetic current of width s is placed on the central plane inside the rectangular dielectric with width W and hight $2H$.

The PCMM is applied to the structure of Fig.2(b), and the directive pattern has been calculated. Also, HFSS is applied to the structure of Fig.2(a) to obtain the directive pattern for comparison. The HFSS is only available to the analysis of finite space, hence the conducting plate of Fig.2(a) is replaced by the finite $(3.3\lambda_0\times 3.3\lambda_0)$ conducting plate in this analysis. The dielectric is homogeneous and of the relative permittivity of $\varepsilon_r=4$.

Fig.3 (a)∼(d) are the directive patterns for the structures with dielectric width $W=0.5\lambda_0$, hight $H=0.5\lambda_0$ and the slot width $s=0.1\lambda_0$, and the slot position x_0 from $0, 0.1\lambda_0, 0.125\lambda_0, 0.2\lambda_0$ from the center. They are normalized by the respective maximum value. There is a relatively good coincidence between the PCMM and the HFSS, including the behavior of the null point movement accompanying the slot position change. However, there seems to be about 10dB difference near $\theta=-90^\circ, 90^\circ$ caused by the different models of the conducting plate which is infinite in the PCMM and finite in the HFSS.

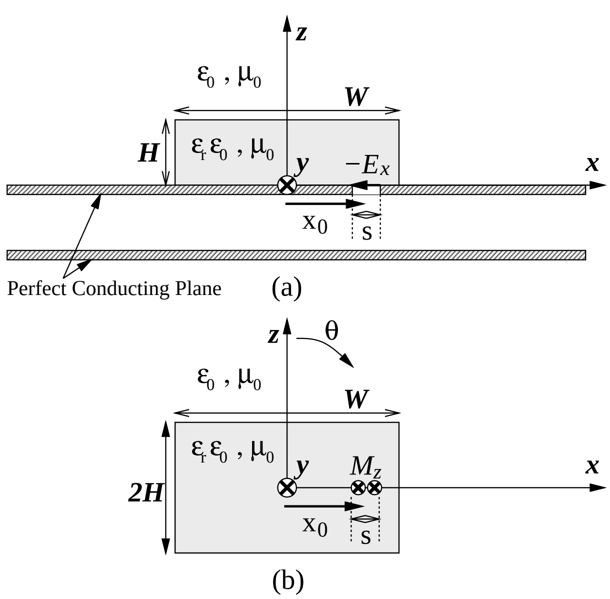

Figure 2: Dielectric loaded slot antenna

4 Conclusion

This paper described how the PCMM is applied to the numerical analysis of antennas consisting of dielectric materials. An example for the TE^y incident dielectric cylinder of infinite extent is given with some care which has to be paid in the application. It has been confirmed that the PCMM has several merits over the existing analytical method. First, it does not produce an non-physical solution of resonance, which is peculiar to the boundary element method for the problem treating dielectric. Secondly, the form of the integral equation keeps the same form irrespective to the position of the source, inside or outside of the dielectric, hence the program coding can effectively be done.

Although this paper treated only the 2D problems, it is expected that the 3D problems will also be treated with the similar merits and conveniences as in the 2D problem, and will be applied for the design of the next generation high frequency antennas.

References

[1] J. H. Richmond : " Scattering by a dielectric cylinder of arbitrary cross section shape," IEEE Trans. Antennas Propag., vol. AP-13, 3, pp.334-341, 1965.

[2] J. H. Richmond : " TE-Wave scattering by a dielectric cylinder of arbitrary cross-section shape," IEEE Trans. Antennas Propag., vol. AP-14, 4, pp.460-464, 1966.

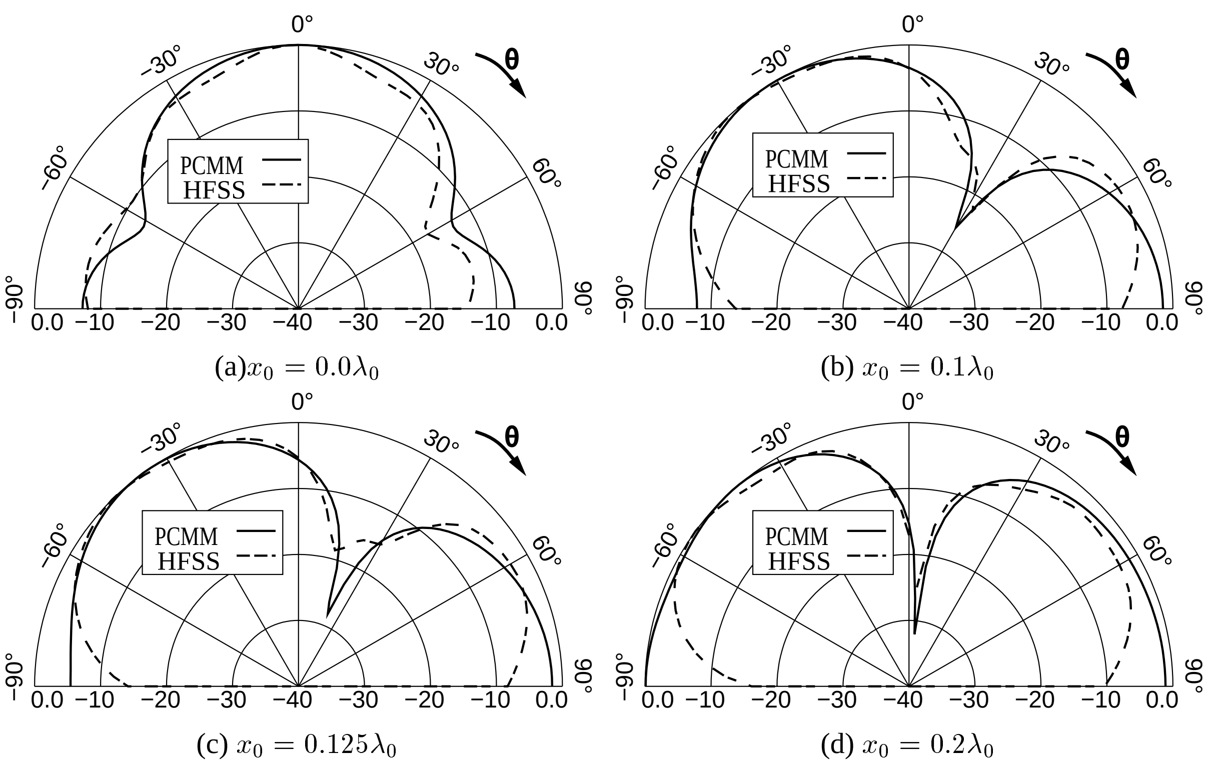

Figure 3: Change of directive patterns in dB, when slot position changed ($W = H = 0.5\lambda_0$)